Gravitational Collapse and Black Holes

Diogo Silva (n.56845)[1]

[1]*Centro de Astrofísica e Gravitação - CENTRA, Departamento de Física, Instituto Superior Técnico - IST, Universidade de Lisboa - UL, Av. Rovisco Pais 1, 1049-001 Lisboa, Portugal, email: diogo.l.silva@tecnico.ulisboa.pt*

To study the gravitational collapse one must solve the Einstein field equations with the appropriate mass energy distribution. While such is a very complex task, tools have been devised to make the analytical solution easier to obtain. In this work we solve the simpler models of stars and thin shells made of dust using junction conditions. We obtain a closed form describing their collapse and describe the evolution of the collapse through its features, namely the formation of the apparent and event horizons as well as the congruence of null geodesics. We also evaluate the limiting cases of the trajectories of the bound and unbound thin shells and show them to approximate those of spherical ingoing flashes of light.

I. INTRODUCTION

The phenomena of gravitational collapse and subsequent formation was a remarkable and non trivial consequence of Einstein's general theory of relativity, first published in 1915 [1]. Despite the inherent intractability of the field equations, the first solution to the field equations, obtained by Schwarzschild, came just one year after [2]. Assuming the source to be non rotating, static and spherically symmetric, the resulting line element, in coordinates (t, r, θ, ϕ), is

$$\mathrm{d}s^2 = -V(r)\mathrm{d}t^2 + V^{-1}(r)\mathrm{d}r^2 + r^2\mathrm{d}\Omega^2\,, \qquad (1)$$

where $V(r) = \left(1 - \frac{2GM}{c^2 r}\right)$ and $\mathrm{d}\Omega^2 = \mathrm{d}\theta^2 + \sin^2\theta\,\mathrm{d}\phi^2$, with M being a constant of motion identified with the mass of the point source. The line element of Eq. (1) shows two singularities, at $r = 0$ and at the Schwarzcshild radius $r = r_S = \frac{2GM}{c^2}$. The latter is seen to be a coordinate singularity, removable by an appropriate coordinate transformation. However, the singularity at $r = 0$ and the shift of the t and r coordinate in the region $r < r_S$ was unusual behaviour.

By 1939 it was known that a star of sufficient mass could not develop a neutron star [3]. To approach this problem, Oppenheimer and Snyder [4] modeled the collapsing star as a sphere of dust, i.e. of pressureless material, and left it to contract. A collapsing spherical body does not emit gravitational waves, and no other form of ejecta, either of matter or radiation, was considered. Consequently, the exterior region was vaccum, and amenable to the Schwarzschild solution. For the interior, they used a collapsing cosmological model previously developed by Tolman [5].

One may note the assumption of a distribution of dust does not present a serious simplification, as the forces due to pressure could always be considered non critical, should the star be taken to be massive enough. As a result, the star was found to contract continuously, going towards the singularity at the center in finite time. Any observer that fell with the star, beyond the spacelike surface of Schwarzschild radius, was found trapped and unable to communicate with the exterior. Such an object would later come to be known as a black hole [6] and their existence confirmed by observations of the Event Horizon Telescope [7].

Since then, gravitational collapse has been used extensively to probe emergent features of gravitation. One example of this can be seen in the exposition in the book by Novikov and Frolov [8] on the features of black and white holes, where Lemaître and Eddington-Finkelstein coordinate systems are used to understand the nature of the event horizon and the singularity at the center. For another example see the work of Joshi, Dadhich and Marteens [9] on the formation of naked singularities in general relativity in marginally bounded collapse, later expanded for all cases by Mena, Nolan and Tavakol [10].

Notably, collapsing bodies have been used to unfold the very process of black hole formation. Choptuik [11] showed a scalar field minimally coupled to the field equations, considering non rotation and spherical symmetry, would give rise to self-similar solutions, i.e. solutions invariant up to a scale factor. On total contraction, the scalar field would lead to a phase transition related to the parameter governing the strength of the gravitational interactions, p. Above a critical value p_c, the black hole properties would respect a power law, $M_{BH} = |p - p_c|^\gamma$, with γ a universal exponent. Thus, it was understood the properties of the black hole and the conditions for its formation could be explicitly established. The study of critical collapse would be expanded to cover different initial conditions and alternative theories of gravity. For an overview, see the review by Gundlach and Martín-García [12]. For an example, see the work by Rocha and Tomašević [13] on critical collapse in Einstein-Maxwell-dilaton theories.

Despite the fruitfulness of gravitational collapse as a tool to study general relativity, it was marred with technical difficulties. Solving the field equations for one spacetime composed of two distinct regions, each with its own energy matter distribution, presented an extremely complex analytical problem. To solve this issue, a set of junction conditions was developed independently by Darmois [14], Misner and Sharp [15] and by Israel [16]. In

brief, one considers the spacelike surface separating the two regions, and defines for each region a distinct spacetime. Then, applying the junction conditions, one gets the equations governing the dynamics of the system.

The junction conditions are a powerful set of tools that greatly ease the task of extracting the dynamics out of a given problem. However, they also allow new models to be considered. Of particular interest is the thin shell model, where the energy matter distribution is restricted to a shell of infinitesimal width. The localized distribution further simplifies the mathematical complexity, while not compromising the validity of the results. Thus, thin shells have seen wide adoption in studies on gravitational collapse. See for example the work by Adler, Bjorken, Chen and Liu [17] where light shells are used to study the formation of black and white holes. For another example, see the work by Lynden-Bell and Lemos [18] on the extension of Newtonian self-similar solutions of Penston to general relativity, later generalized to accommodate the unbound and bound collapse [19]. Rebounding thin shells have also been used by Israel [20] to study asymmetric collapse.

The modern definition of the junction conditions, and the one we will be using, is the one relying on a distributional formalism. This can be found in the book by Poisson [21].

Going forward, the paper is organized as follows. In section II detail the region exterior to the collapsing body. The next sections are dedicated to defining the interior region, particular to the system, and initial conditions, at hand. As such, in section III we study spherically symmetric collapsing stars made of homogeneous distributions of dust in the marginally bound, unbound and bound cases. In section IV we study collapsing spherically symmetric thin shells made of dust in the marginally bound, unbound and bound cases. In section V we finalize with the concluding remarks and possible venues for future work. In this paper we use natural units, i.e. $c = G = 1$, and the metrics have signature $(-,+,+,+)$.

II. EXTERIOR REGION

We assume the collapsing body is non rotating and spherically symmetric. Additionally, we assume no matter or radiation is ejected during contraction so that the exterior region is vacuum. As such, Birkhoff's theorem states this region must be a Schwarzschild spacetime. The metric is then of the form of Eq. (1),

$$\mathrm{d}s^2 = -V(r)\mathrm{d}\,t^2 + V^{-1}(r)\,\mathrm{d}r^2 + r^2\,\mathrm{d}\Omega^2\,, \tag{2}$$

with $V(r) = \left(1 - \frac{2M}{r}\right)$ and $\mathrm{d}\Omega^2 = \mathrm{d}\theta^2 + \sin^2\theta\,\mathrm{d}\phi^2$. The Schwarzschild radius is $r = 2M$ and the null geodesics are described by the equation

$$t = t_0 \pm \left(r - r_0 + \ln\left|\frac{r-2M}{r_0-2M}\right|\right)\,, \tag{3}$$

with the plus sign for outgoing null geodesics and the minus sign for the ingoing null geodesics, respectively. Henceforth, the surface of the collapsing body, star or shell, will be denoted by the coordinates (T, R).

III. COLLAPSING STARS

For collapsing stars, we take the energy matter distribution to be homogeneous. The material is dust, i.e., pressureless matter. The corresponding energy matter tensor is

$$T^{\alpha\beta} = \rho_0\, u^\alpha u^\beta\,, \tag{4}$$

with ρ_0 the energy density of the star and $u^\alpha = \frac{\mathrm{d}x^\alpha}{\mathrm{d}\tau}$ its 4-velocity field, τ being the proper time.

For the junction conditions we define the normal over the surface of separation n_α and the induced coordinate basis vectors $e^\alpha{}_a = \frac{\mathrm{d}x^\alpha}{\mathrm{d}y^a}$, with x^α the exterior coordinate and y^a the induced coordinate. We now note there is no infinitesimal surface energy matter distribution. As such, we have to impose

$$[h_{ab}] = 0\,, \tag{5}$$

$$[K_{ab}] = 0\,, \tag{6}$$

where square brackets denote the jump of a quantity over a surface of separation, $h_{ab} = g_{\alpha\beta}\, e^\alpha{}_a e^\beta{}_b$ is the induced metric over the surface and $K_{ab} = n_{\alpha\beta} e^\alpha{}_a e^\beta{}_b$ is the extrinsic curvature. Thus, Eq. (5) relates to the continuity of the metric over the surface, and Eq. (6) to the continuity of the extrinsic curvature over the surface. We now proceed to solve both these junction conditions, Eqs. (5) and (6), when the exterior metric, Eq. (2), is coupled to an interior metric suitable to the initial conditions. The metric chosen will be, comoving with the collapsing star, specifically of the Friedmann-Lemaître-Robertson-Walker (FLRW) type,

$$\mathrm{d}s^2 = -\mathrm{d}\tau^2 + \xi^2(\tau)\left[\frac{\mathrm{d}a^2}{1-k\,a^2} + a^2\,\mathrm{d}\Omega^2\right]\,, \tag{7}$$

where $\xi(\tau)$ is the scale factor, k is the curvature of space and $a \in [0, A]$ is the radial coordinate. The parameter k can take the values -1, 0 and 1 for negative, zero and positive curvature respectively, and will be chosen according to the case at hand.

A. $k = 0$: Marginally Bound Case

For the marginally bound case we choose a FLRW metric, Eq. (7), with k=0,

$$\mathrm{d}s^2 = -\mathrm{d}\tau^2 + \xi^2(\tau)\left[\mathrm{d}a^2 + a^2\,\mathrm{d}\,\Omega^2\right]\,, \tag{8}$$

Applying the junction conditions, Eqs. (5) and (6), with the pair of metrics, yields the relations

$$1 = \left(1 - \frac{2M}{R}\right)\dot{T}^2 - \left(1 - \frac{2M}{R}\right)^{-1}\dot{R}^2\,, \tag{9}$$

$$\ddot{R} = -\frac{M}{R^2}\,, \tag{10}$$

$$\xi(\tau)A = R\,. \tag{11}$$

The trajectory in proper time can be directly obtained by solving Eq. (10)

$$\tau(R) = \frac{2}{3}\left(\frac{R_0^3}{2M}\right)^{1/2}\left[1 - \left(\frac{R}{R_0}\right)^{3/2}\right], \tag{12}$$

with $R_0 \equiv R(0)$. It is, however, worthwhile to search for a parameter such that the metric of Eq. (8) takes a simpler form. Take η such that the relation of Eq. (10) gives rise to the set of differential equations

$$\frac{\partial R}{\partial \eta} = -\frac{1}{A}(2MR)^{1/2}\,, \tag{13}$$

$$\frac{\partial \tau}{\partial \eta} = \frac{R}{A}\,, \tag{14}$$

which give the simple parametric description of the trajectory of the star's surface

$$R(\eta) = \frac{1}{4}2M\left(\frac{\eta}{A}\right)^2\,, \tag{15}$$

$$\tau(\eta) = \frac{1}{12}2M\left(\frac{\eta}{A}\right)^3\,. \tag{16}$$

Furthermore, with the parameter η and the junction relation for the scale factor, Eq. (11), the metric, Eq. (8) takes the form

$$\mathrm{d}s^2 = \xi^2(\eta)[-\mathrm{d}\eta^2 + \mathrm{d}a^2 + a^2\,\mathrm{d}\Omega^2]\,, \tag{17}$$

with the scale factor given by

$$\xi(\eta) = \frac{2M}{4A}\left(\frac{\eta}{A}\right)^2\,. \tag{18}$$

The new metric, Eq. (17), provides a simple relation for null geodesics. In fact, null geodesics are given by diagonal lines like is characteristic of the Kruskal-Szekeres coordinate system. This allows a clearer picture of the sequence of events during gravitational collapse.

For the trajectory as described by an external observer, we turn to the results of the junction conditions, Eqs. (9) and (10), from which we get

$$T(R) = T_0 - \frac{2}{3}\left(\frac{R}{2M}\right)^{1/2}(R + 6M) + \\ + 2M\ln\left|\frac{R^{1/2} + (2M)^{1/2}}{R^{1/2} - (2M)^{1/2}}\right|. \tag{19}$$

The event horizon is obtained by considering the null geodesic crossing the surface when $R = \xi(\eta^{EH})A = 2M$. Doing so, we obtain

$$\eta^{EH} = -3A + a\,, \tag{20}$$

and the apparent horizon can be obtained by using the method of Eardley and Smarr [22]

$$(\nabla g_{22}) \cdot (\nabla g_{22}) = 0\,, \tag{21}$$

from which we find

$$\eta^{AH} = -2a\,. \tag{22}$$

With all the elements here obtained, we can build the causal structure of each spacetime, Figures 1a and 1b. For the exterior region we use a Kruskal-Szekeres coordinate system, allowing for some compatibility in both structures and for the sake of clarity.

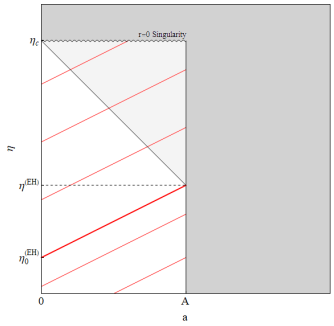

(a) Interior Causal Structure.

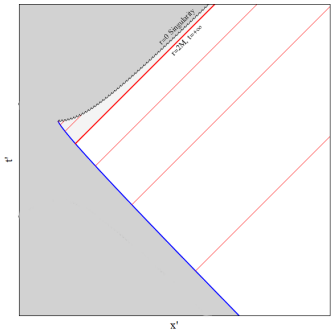

(b) Exterior Causal Structure.

FIG. 1: The causal structure of the (1a) interior and (1b) exterior spacetimes in coordinate systems where null geodesics are diagonal straight lines. The outgoing light rays are shown in thin red lines, with the event horizon being the thick red line. The apparent horizon is shown with a thin black line, the singularity with a undulating black line and the trajectory of the surface of the collapsing star with a thick blue line. The light shaded region represents the region of trapped surfaces and the dark shaded region does not belong to the spacetime and is non physical.

B. $k = -1$: Unbound Case

For the unbound case we choose a FLRW metric, Eq. (7), with $k = -1$,

$$\mathrm{d}s^2 = -\mathrm{d}\tau^2 + \xi^2(\tau)\left[\frac{\mathrm{d}a^2}{1+a^2} + a^2\,\mathrm{d}\Omega^2\right]. \tag{23}$$

Applying the juntion conditions, Eqs. (5) and (6), with the pair of metrics, yields the relations

$$1 = \left(1 - \frac{2M}{R}\right)\dot{T}^2 - \left(1 - \frac{2M}{R}\right)^{-1}\dot{R}^2\,, \tag{24}$$

$$\dot{R}^2 = A^2 + \frac{2M}{R}\,, \tag{25}$$

$$\xi(\tau)A = R\,. \tag{26}$$

From the second, Eq. (25), one finds immediately the relation for the initial velocity $\lim_{R\to\infty}\dot{R} = v_{R\to\infty} = = -A$. Take $v_0 = A$. The pair of Eqs. (24) and (25) relate the coordinates τ, T and R, and thus can be used to obtain the trajectory. The solution can also be obtained in a compact form by taking a parameter η such that

$$\frac{\partial R}{\partial \eta} = -\frac{R}{v_0}\left(v_0^2 + \frac{2M}{R}\right)^{1/2}, \tag{27}$$

$$\frac{\partial \tau}{\partial \eta} = \frac{R}{v_0}\,, \tag{28}$$

with which we get the description for the trajectory of the star's surface

$$R(\eta) = \frac{M}{v_0^2}(\cosh\eta - 1)\,, \tag{29}$$

$$\tau(\eta) = \frac{M}{v_0^3}(\sinh\eta - \eta)\,. \tag{30}$$

Furthermore, with the parameter η and the junction relation for the scale factor, Eq. (26), the metric, Eq.(23), takes the form

$$\mathrm{d}s^2 = \xi^2(\eta)\left[-\mathrm{d}\eta^2 + \frac{\mathrm{d}a^2}{1+a^2} + a^2\,\mathrm{d}\Omega^2\right], \tag{31}$$

with the scale factor given by

$$\xi(\eta) = \frac{M}{v_0^3}(\cosh\eta - 1)\,. \tag{32}$$

The new metric, Eq. (31), gives a simpler relation to the null geodesics, and allows a clearer picture of the sequence of events during gravitational collapse.

For the trajectory as described by an external observer, we turn to the results of the junction conditions, Eqs. (24) and (25), with $A = v_0$. Doing so, we obtain

$$\frac{\mathrm{d}T}{\mathrm{d}R} = -\left(1 - \frac{2M}{R}\right)^{-1}\left(\frac{v_0^2 R + R}{v_0^2 R + 2M}\right)^{1/2}, \tag{33}$$

from which we get

$$\begin{aligned} T(R) = T_0 &- \frac{1}{v_0^2}[R\epsilon\Phi(R)]^{1/2} + \\ &+ 2M\ln\left|\frac{(\epsilon R)^{1/2} + \Phi^{1/2}(R)}{(\epsilon R)^{1/2} - \Phi^{1/2}(R)}\right| + \\ &+ \frac{2M\epsilon^{1/2}(1-2v_0^2)}{v_0^3}\ln\left(\frac{v_0 R^{1/2} + \Phi^{1/2}(R)}{(2M)^{1/2}}\right), \end{aligned} \tag{34}$$

where $\epsilon = 1 + v_0^2$ and $\Phi(R) = 2M + v_0^2 R$. The event horizon is obtained by solving the equation for the null geodesics

$$\frac{\partial \eta}{\partial a} = \pm\frac{1}{(1+a^2)^{1/2}}\,, \tag{35}$$

with the plus sign for the outgoing null geodesics and the minus for ingoing null geodesics. Considering the event horizon to be the ougoing null geodesics crossing the surface when $R = \xi(\eta^{EH})A = 2M$, we get

$$\eta^{EH} = -\mathrm{arccosh}(2v_0^2) - \mathrm{arcsinh}v_0 + \mathrm{arcsinh}a\,, \tag{36}$$

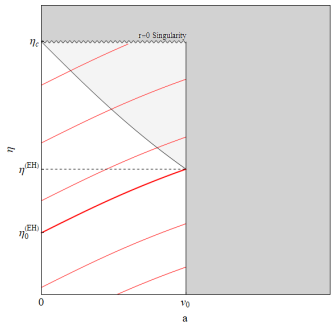

(a) Interior Causal Structure.

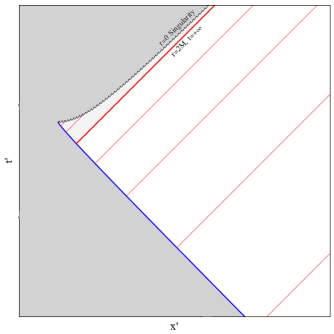

(b) Exterior Causal Structure.

FIG. 2: The causal structure of the (2a) interior and (2b) exterior spacetimes. The outgoing light rays are shown in thin red lines, with the event horizon being the thick red line. The apparent horizon is shown with a thin black line, the singularity with a undulating black line and the trajectory of the surface of the collapsing star with a thick blue line. The light shaded region represents the region of trapped surfaces and the dark shaded region does not belong to the spacetime and is non physical.

and the apparent horizon can be obtained using once more the algorithm by Eardley and Smarr

$$(\nabla g_{22}) \cdot (\nabla g_{22}) = 0\,, \tag{37}$$

from which we find

$$\eta^{AH} = -\text{arccosh}(2a^2 + 1)\,. \tag{38}$$

With all the elements here obtained, we can build the causal structure of each spacetime, Figures 2a and 2b. For the exterior region we use a Kruskal-Szekeres coordinate system, allowing for some compatibility in both structures for the sake of clarity.

C. $k = 1$: Bound Case

For the bound case we choose a FLRW metric, Eq. (7), with $k = 1$,

$$\mathrm{d}s^2 = -\mathrm{d}\tau^2 + \xi^2(\tau)\left[\frac{\mathrm{d}a^2}{1-a^2} + a^2\,\mathrm{d}\Omega^2\right]\,. \tag{39}$$

Applying the junction conditions, Eqs. (5) and (6), with the pair of metrics, yields the relations

$$1 = \left(1 - \frac{2M}{R}\right)\dot{T}^2 - \left(1 - \frac{2M}{R}\right)^{-1}\dot{R}^2\,, \tag{40}$$

$$\dot{R}^2 = -A^2 + \frac{2M}{R}\,, \tag{41}$$

$$\xi(\tau)A = R\,. \tag{42}$$

From the second, Eq. (41), one immediately finds the relation $A = -\left(\frac{2M}{R_0}\right)^{1/2}$. The pair of Eqs. (40) and (41) relate the coordinates τ, T and R, and thus can be used to obtain the trajectory. The solution can also be obtained in a compact form by taking a parameter η such that

$$\frac{\partial R}{\partial \eta} = -R\left[\frac{R_0}{2M}\left(\frac{2M}{R} - \frac{2M}{R_0}\right)\right]^{1/2} \tag{43}$$

$$\frac{\partial \tau}{\partial \eta} = R\left(\frac{R_0}{2M}\right)^{1/2}\,, \tag{44}$$

with which we get the description for the trajectory of the star's surface

$$R(\eta) = \frac{R_0}{2}(1 + \cos\eta)\,, \tag{45}$$

$$\tau(\eta) = \frac{R_0}{2}(\eta + \sin\eta)\,. \tag{46}$$

With the parameter η and using Eq. (42), the metric of Eq. (39) takes the form

$$\mathrm{d}s^2 = \xi^2(\eta)\left[-\mathrm{d}\eta^2 + \frac{\mathrm{d}a^2}{1-a^2} + a^2\,\mathrm{d}\Omega^2\right]\,, \tag{47}$$

with the scale factor given by

$$\xi(\eta) = \frac{R_0}{2}\left(\frac{R_0}{2M}\right)^{1/2}(1 + \cos\eta)\,. \tag{48}$$

The new metric, Eq. (47) gives a simpler relation to the null geodesics, and thus allows a clearer picture of the sequence of events during gravitational collapse.

For the trajectory as described by an external observer, we turn to the results of the junction conditions, Eqs. (40) and (41), taking for A its relation with R_0. Doing so, we get

$$\frac{\mathrm{d}T}{\mathrm{d}R} = -\left(1 - \frac{2M}{R}\right)^{-1}\left(\frac{R(R_0 - 2M)}{2M(R_0 - R)}\right)^{1/2}\,, \tag{49}$$

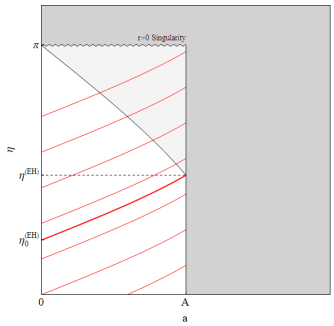

(a) Interior Causal Structure.

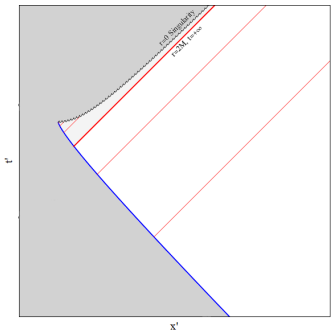

(b) Exterior Causal Structure.

FIG. 3: The causal structure of the (3a) interior and (3b) exterior spacetimes. The outgoing light rays are shown in thin red lines, with the event horizon being the thick red line. The apparent horizon is shown with a thin black line, the singularity with a undulating black line and the trajectory of the surface of the collapsing star with a thick blue line. The light shaded region represents the region of trapped surfaces and the dark shaded region does not belong to the spacetime and is non physical.

from which we get

$$T(R) = T_0 + \left[\frac{R\Delta(R_0-R)}{2M}\right]^{1/2} - \\ - (2M\Delta)^{1/2}\,\frac{R_0+4M}{4M}\arccos\left(\frac{R_0-2R}{R_0}\right) + \\ +2M\ln\left|\frac{4[MR\Delta(R_0-R)]^{1/2} - 2^{1/2}\Theta(R)}{2^{1/2}R_0(R-2M)}\right|, \quad (50)$$

where $\Delta = R_0 - 2M$ and $\Theta(R) = 4MR + 2MR_0 - RR_0$. The event horizon is obtained by solving the equation of the null geodesics

$$\frac{\partial\eta}{\partial a} = \pm\frac{1}{(1-a^2)^{1/2}}\,, \quad (51)$$

with the plus sign for ougoing null geodesics and the minus for ingoing null geodesics. Considering the event horizon to be the outgoing null geodesic crossing the surface when $R = \xi(\eta^{EH})A = 2M$, we get

$$\eta^{EH} = \arccos\left(\frac{2M-\Delta}{R_0}\right) - \arcsin A + \arcsin a\,, \quad (52)$$

and the apparent horizon can be obtained using once again

$$(\nabla g_{22})\cdot(\nabla g_{22}) = 0\,, \quad (53)$$

from which we find

$$\eta^{AH} = \arccos\left(2a^2-1\right). \quad (54)$$

With all the elements here obtained, we can build the causal structure of each spacetime, Figures 3a and 3b. For the exterior region we use a Kruskal-Szekerers coordinate system, allowing for some compatibility in both structures and for the sake of clarity.

IV. COLLAPSING THIN SHELLS

For collapsing thin shells, we take the energy matter distribution to be spherically symmetric and localized at the surface. The material is again dust, i.e. pressureless matter. The corresponding energy matter tensor is

$$T^{\alpha\beta} = \sigma\,u^\alpha\,u^\beta\,\delta(r-R)\,, \quad (55)$$

with σ the energy density of the shell, $u^\alpha = \frac{\mathrm{d}x^\alpha}{\mathrm{d}\tau}$ its 4-velocity field, with τ being the proper time and $\delta(r-R)$ the delta function. We thus have $S^{\alpha\beta} = \sigma\,u^\alpha\,u^\beta$.

For the junction conditions we define again the normal over the surface of separation n^α, and the induced coordinate basis vectors $e^\alpha_{\ a} = \frac{\mathrm{d}x^\alpha}{\mathrm{d}y^a}$. Since now the energy matter distribution is localized completely on the surface, the junction conditions are now

$$[h_{ab}] = 0\,, \quad (56)$$

$$S_{ab} = -\frac{1}{8\pi}\left([K_{ab}] - [K]h_{ab}\right), \quad (57)$$

where we now also have $S_{ab} = S_{\alpha\beta}\,e^\alpha_{\ a}\,e^\beta_{\ b}$ and the trace of the extrinsic curvature tensor, $K = K^a_{\ a} = h^{ab}K_{ab}$. The first junction condition, Eq. (56), still pertains to continuity of the metric over the surface. The second junction condition, Eq. (57), now states the extrinsic curvature is subject to a discontinuity induced by the surface distribution. The solution to both junction conditions, Eqs. (56) and (57), can be obtained after coupling the exterior metric, Eq. (2), to a suitable metric describing the interior. As the interior of the shell is vacuum, the interior region must be a flat spacetime. As such the suitable metric, for thin shells of any energy, is the Minkowski metric

$$\mathrm{d}s^2 = -\mathrm{d}t_-^2 + \mathrm{d}r_-^2 + r_-^2\,\mathrm{d}\Omega^2\,, \quad (58)$$

where $r_- \in [0, R]$. Now the proper time corresponds to that of an observer falling with the surface of the shell. With the exterior and interior metrics being uniquely defined, we find from the continuity of the metric

$$1 = \dot{T_-}^2 - \dot{R}^2 = \\ = \left(1-\frac{2M}{R}\right)\dot{T}^2 - \left(1-\frac{2M}{R}\right)^{-1}\dot{R}^2\,, \quad (59)$$

and from the discontinuity of the extrinsic curvature

$$M = m\left(\dot{R}^2+1\right)^{1/2} - \frac{m^2}{2R}\,, \quad (60)$$

where $m = 4\pi R^2\sigma$ is a constant of motion. M, the mass parameter of Schwarzschild spacetime, can thus be identified with the energy of the system. Inverting the equation of motion, Eq. (60), we find

$$\dot{R} = \pm\left(\frac{M^2}{m^2} + \frac{M}{R} + \frac{m^2}{4R^2} - 1\right)^{1/2}, \quad (61)$$

where the plus sign corresponds to an expanding thin shell, and the minus a contracting thin shell. It is immediate, from the limits $\dot{R}\to 0$ and $R\to\infty$ the bound case corresponds to $0 < M < m$, the marginally bound case to $M = m$ and the unbound case to $M > m$. We will now study the solution to each case.

A. $M = m$: Marginally Bound Case

For the marginally bound case we choose $M = m$, with which Eq. (61) gives

$$\dot{R} = -\left(\frac{M}{R} + \frac{M^2}{4R^2}\right)^{1/2}, \quad (62)$$

from which we get the solution to the trajectory with respect to the proper time

$$\tau(R) = -\frac{M}{6} + \frac{1}{6}\left(1-\frac{2M}{R}\right)[M(M+4R)]^{1/2}. \quad (63)$$

We must consider additionally the solution as seen by an observer in the interior region, i.e. in the Minkowski spacetime. We can obtain the differential equation by using the result from the continuity of the metric, Eq. (59), on Eq. (62). Doing so, we find

$$\frac{\mathrm{d}T_-}{\mathrm{d}R} = -\left(\frac{4R^2+4MR+M^2}{4MR+M^2}\right)^{1/2}, \tag{64}$$

which can be solved to give

$$T_-(R) = \frac{M}{3} - \frac{1}{3}\left(1+\frac{R}{M}\right)[M(M+4R)]^{1/2}. \tag{65}$$

The same method may be used to obtain the solution as seen by an observer in the exterior region, i.e. the Schwarzschild spacetime. We find

$$\frac{\mathrm{d}T}{\mathrm{d}R} = -\left(1-\frac{2M}{R}\right)^{-1}\left(\frac{4R^2-4MR+M^2}{4MR+M^2}\right)^{1/2}, \tag{66}$$

from which the solution follows

$$\begin{aligned} T(R) = {} & \frac{4M}{3} - \frac{1}{3}(R+4M)\left(1+\frac{4R}{M}\right)^{1/2} + \\ & + 2M\ln\left|\frac{1}{2}\frac{3M^{1/2}+(M+4R)^{1/2}}{3M^{1/2}-(M+4R)^{1/2}}\right|. \end{aligned} \tag{67}$$

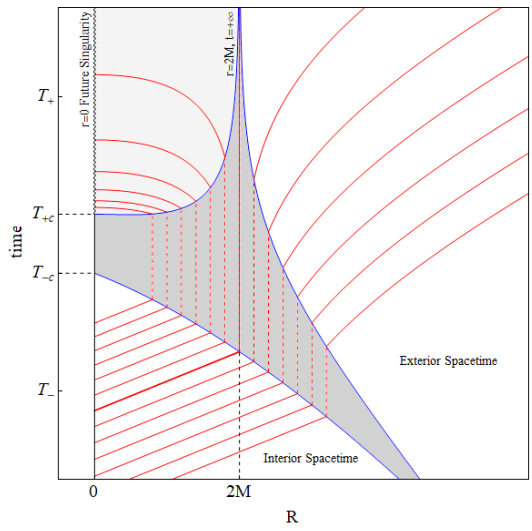

FIG. 4: The causal structure of spacetime for $M = m$ in exterior Schwarzschild coordinates and interior Minkowski. The trajectory of the shell is the blue line. In red are drawn the outgoing null rays, with the last one reaching infinity, shown in a thicker line, corresponding to the event horizon. The light shaded region is the region of trapped surfaces and the spacelike surface delimiting it, interior to the event horizon, corresponds to the apparent horizon. The dark shaded region is non physical and is used to separate the two different spacetimes. The singularity is the endpoint of the evolution and is shown in a curvilinear line.

We now consider the event horizon. Since the interior is a flat spacetime, light rays follow along straight lines. Since the event horizon corresponds to the light ray crossing the surface when $R = 2M$, its description is simply

$$t_-^{EH} = r_- - \frac{14M}{3}. \tag{68}$$

As the apparent horizon is defined as the boundary of trapped surfaces [23], we modify the method by Eardley and Smarr, which depends on the transition of the normal to a null vector, to be such that

$$(\nabla g_{22})\cdot(\nabla g_{22})\Big|_{r\to R^+} \leq 0, \tag{69}$$

from which we find the surface of shell, after crossing the event horizon, to define the apparent horizon.

With all the elements here obtained, we can build the causal structure of the whole spacetime, integrated into one diagram, Figure 4.

B. $M > m$: Unbound Case

For the unbound case we choose $M > m$, with which Eq. (61) gives

$$\dot{R} = -\left(\frac{M^2}{m^2} - 1 + \frac{M}{R} + \frac{m^2}{4R^2}\right)^{1/2}, \tag{70}$$

which is valid for all R. In the limit $R\to\infty$ we find $v_0 = \lim_{R\to\infty}\dot{R} = -\left(\frac{M^2}{m^2}-1\right)^{1/2}$. The solution to Eq. (70) with respect to the proper time is

$$\begin{aligned} \tau(R) = {} & \frac{m^3}{2\epsilon^2}\Big(1 - \frac{1}{m^2}\Phi(R) + \\ & + \frac{M}{\epsilon}\ln\left[\frac{m^2M+2\epsilon^2R+\epsilon\Phi(R)}{m^2(M+\epsilon)}\right]\Big), \end{aligned} \tag{71}$$

where $\epsilon = (M^2-m^2)^{1/2}$ and $\Phi(R) = [m^2(m^2+4MR) + +4\epsilon^2R^2]^{1/2}$. The description for the trajectory of the shell, as seen by an observer in the interior region can be obtained, like before, by applying the condition on the continuity of the metric, Eq. (59), to Eq. (70), giving

$$\frac{\mathrm{d}T_-}{\mathrm{d}R} = -\left(\frac{4M^2R^2+4Mm^2R+m^4}{4\epsilon^2R^2+4Mm^2R+m^4}\right)^{1/2}, \tag{72}$$

from which follows

$$\begin{aligned} T_-(R) = {} & \frac{m^2M}{2\epsilon^2}\Big(1 - \frac{\Phi(R)}{m^2} + \\ & + \frac{m^2}{M\epsilon}\ln\left[\frac{m^2M+2\epsilon^2R+\epsilon\Phi(R)}{m^2(M+\epsilon)}\right]\Big). \end{aligned} \tag{73}$$

The same method may be used to obtain the description of the trajectory as seen by an observer in the exterior

region. We find

$$\frac{\mathrm{d}T}{\mathrm{d}R} = -\left(1-\frac{2M}{R}\right)^{-1}\left(\frac{4M^2R^2-4Mm^2R+m^4}{4\epsilon^2R^2+4Mm^2R+m^4}\right)^{1/2}, \tag{74}$$

which admits the solution

$$T(R) = -\frac{M}{2\epsilon^2}\Bigg(\Phi(R) - m^2 + \\ + \frac{4M^4-6M^2m^2+m^4}{M\epsilon}\ln\left[\frac{Mm^2+2\epsilon^2R+\epsilon\Phi(R)}{m^2(\epsilon+M)}\right] - \\ -4\epsilon^2\ln\left|\frac{m^2\Xi(R)+(4M^2-m^2)[2MR+\Phi(R)]}{4Mm^2(R-2M)}\right|\Bigg), \tag{75}$$

with $\Xi(R) = 4M^2 - 4MR + m^2$. The trajectories described by Eq. (75) are show in Figure 5 for various values of the ratio M/m.

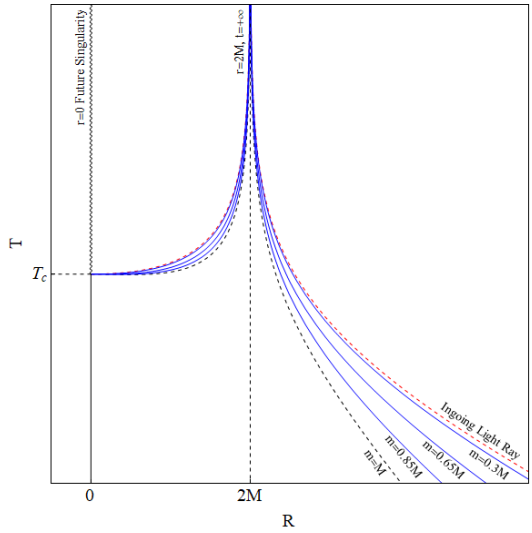

FIG. 5: With blue lines, the unbound thin shell collapse in exterior Schwarzchild coordinates for different values of the shell's rest mass, m, relative to its energy parameter M. The dashed black line represents the trajectory of the marginally bound collapsing shell, studied in section IV A. The dashed red line represents an ingoing null geodesic.

It is seen that, as the ratio M/m increase, the geodesics approaches the appropriate ingoing null geodesic. Indeed, taking the $m \to 0$ limit of Eq. (75), one finds

$$\lim_{m\to 0} T(R) = -R - 2M\ln\left|\frac{R-2M}{2M}\right|, \tag{76}$$

which is exactly the ingoing geodesic found in section II with $t_0 = r_0 = 0$. In this limit, the shell approaches a converging flash of light, so that the trajectory approaches the respective null geodesic.

The event and apparent horizon follow as was seen for the marginally bound collapsing thin shell. In brief, the event horizon follows along the null geodesic in Minkowski space, i.e. a straight line, such that it meets the shell as it crosses $R = 2M$. Thus

$$t_-^{EH} = r_- - 2M - \frac{M(2M^2-m^2)}{\epsilon^2} + \\ + \frac{m^4}{2\epsilon^3}\ln\left[\frac{2M^2-m^2+2M\epsilon}{m^2}\right], \tag{77}$$

while the apparent horizon, from

$$(\nabla g_{22})\cdot(\nabla g_{22})\Big|_{r\to R^+} \leq 0\,, \tag{78}$$

is identified with the trajectory of the shell, after it passes the event horizon. With all the elements here obtained, we can build the causal structure of the whole spacetime, integrated into one diagram, Figure 6.

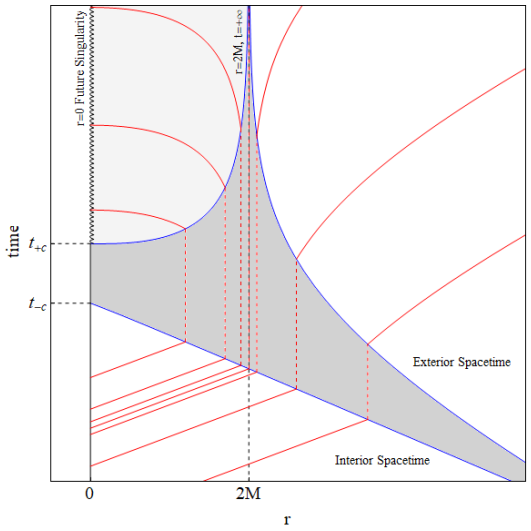

FIG. 6: The causal structure of spacetime for $M > m$, i.e. the unbound case, in exterior Schwarzschild coordinates and interior Minkowski. The trajectory of the shell is the blue line. In red are drawn the outgoing null rays, with the last one reaching infinity, shown in a thicker line, corresponding to the event horizon. The light shaded region is the region of trapped surfaces and the spacelike surface delimiting it, interior to the event horizon, corresponds to the apparent horizon. The dark shaded region is non physical and is used to separate the two different spacetimes. The singularity is the endpoint of the evolution and is shown in a curvilinear line.

C. $M < m$: Bound Case

For the bound case we choose $M < m$, with which Eq. (60) gives

$$\dot{R} = -\left(\frac{M^2}{m^2} - 1 + \frac{M}{R} + \frac{m^2}{4R^2}\right)^{1/2}, \tag{79}$$

which is valid for $R \in [0, R_0]$. The distance from which the shell begins contraction is obtained setting $\dot{R} = 0$. We get $R_0 = \frac{m^2}{2(m-M)}$, which has a minimum of $R_0 = 2M$ at $m = 2M$. Thus there are two regions of interest, those of $M < m < 2M$ and of $m > 2M$. The solution to Eq. (79), with respect to proper time, is

$$\tau(R) = \frac{m}{2\Delta^2}(\Theta(R) - m^2) + \\ + \frac{m^3 M}{2\Delta^3}\left(\arcsin\left[\frac{m^2 M - 2\Delta^2 R}{m^3}\right] - \arcsin\left[\frac{M}{m}\right]\right), \tag{80}$$

where $\Delta = (m^2 - M^2)^{1/2}$ and $\Theta(R) = [m^2(m^2 + 4MR) - \\ - 4\Delta^2 R^2]^{1/2}$. The description for the trajectory of the shell, as seen by an observer in the interior region is obtained by the same method as was done for the unbound contracting thin shell. Thus, applying the condition on the continuity of the metric, Eq. (59), to Eq. (79), we get

$$\frac{\mathrm{d}T_-}{\mathrm{d}R} = -\left(\frac{m^4 + 4M^2R^2 + 4Mm^2R}{m^4 - 4\Delta^2R^2 + 4Mm^2R}\right)^{1/2}, \tag{81}$$

from which follows

$$T_-(R) = \frac{M}{2\Delta^2}(\Theta(R) - m^2) + \\ + \frac{m^4}{2\Delta^3}\left(\arcsin\left[\frac{m^2 M - 2\Delta^2 R}{m^3}\right] - \arcsin\left[\frac{M}{m}\right]\right) \tag{82}$$

Identically, for the description of the trajectory as seen by an observer in the exterior region we find

$$\frac{\mathrm{d}T}{\mathrm{d}R} = -\left(1 - \frac{2M}{R}\right)^{-1}\left(\frac{m^4 + 4M^2R^2 - 4Mm^2R}{m^4 - 4\Delta^2R^2 + 4Mm^2R}\right)^{1/2}, \tag{83}$$

whose solution is

$$T(R) = \pm\frac{1}{2\Delta^2}\Bigg[M(\Theta(R) - m^2) + \\ + \frac{\zeta}{\Delta}\left(\arccos\left[\frac{m^2 M - 2\Delta^2 R}{m^3}\right] - \arccos\left[\frac{M}{m}\right]\right) + \\ + 4M\Delta^2 \ln\left|\frac{m^2\Xi(R) + (4M^2 - m^2)(4MR + \Theta(R))}{4mM(R - 2M)}\right|\Bigg], \tag{84}$$

with $\zeta = m^4 - 6m^2M^2 + 4M^4$, $\Xi(R) = 4M^2 - 4MR + m^2$ and the plus and minus signs for the cases $M < m < 2M$ and $m > 2M$ respectively. The trajectories for these regimes are shown in Figures 7a and 7b respectively.

For the trajectories with $m < 2M$ we find the trajectories to approach those of the marginally bound shell in the limit $m \to M$. however, for $m > 2M$, the trajectories approach those of the ingoing null geodesics in the limit $m \to \infty$. Indeed, in this limit of Eq. (84), we find

$$\lim_{m\to\infty} T(R) = -R - 2M \ln\left|\frac{R - 2M}{2M}\right|, \tag{85}$$

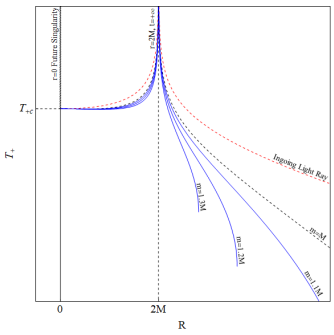

(a) Trajectories for $M < m < 2M$.

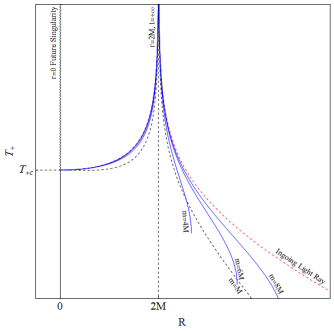

(b) Trajectories for $m > 2M$.

FIG. 7: With blue lines, the bound shell collapse measured in external Schwarzschild time for different values of the rest mass of the shell, m, relative to its energy parameter M. These trajectories can be separated into two categories, those of $M < m < 2M$ in Figure 7a, and those of $m > 2M$ in Figure 7b. The dashed black line represents the trajectory of the marginally bound collapsing shell, studied in chapter IV A. The dashed red line represents an ingoing null geodesic.

which is the equation for ingoing null geodesics found in section II with $t_0 = r_0 = 0$. In this limit, the mass of the shell is such its acceleration is significant. As a consequence, the shell rapidly achieves the limit speed of the light. Then its trajectory approximates that of a converging flash of light.

The event and apparent horizons follow as before. Briefly, the event horizon is given by the null geodesic that touches the shell as it crosses $R = 2M$. Thus

$$t_-^{EH} = r_- - 2M + \frac{M(|m^2 - 4M^2| - m^2)}{2\Delta^2} - \\ - \frac{m^4}{2\Delta^3}\left(\arcsin\left[\frac{M(3m^2 - 4M^2)}{m^3}\right] + \arcsin\left[\frac{M}{m}\right]\right), \tag{86}$$

and the apparent horizon, from

$$(\nabla g_{22}) \cdot (\nabla g_{22})\Big|_{r\to R^+} \leq 0, \tag{87}$$

is identified with the trajectory of the shell after it passes

the event horizon.With all the elements here obtained, we can build the causal structure of the whole spacetime, integrated into one diagram, Figure 8.

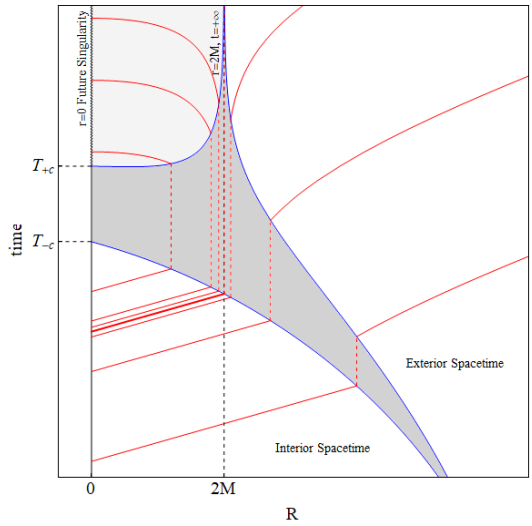

FIG. 8: The causal structure of spacetime for $M < m$, bound case, in exterior Schwarzschild coordinates and interior Minkowski. The trajectory of the shell is the blue line. In red are drawn the outgoing null rays, with the last one reaching infinity, shown in a thicker line, corresponding to the event horizon. The light shaded region is the region of trapped surfaces and the spacelike surface delimiting it, interior to the event horizon, corresponds to the apparent horizon. The dark shaded region is non physical and is used to separate the two different spacetimes. The singularity is the endpoint of the evolution and is shown in a curvilinear line.

V. CONCLUSIONS

In this work we've been able to attest to the power of the junction conditions as a tool to evaluate the gravitational collapse of massive bodies as well as this shells, in the marginally bound, unbound and bound cases. The set of solutions obtained, were done so with simplicity, yet retain generality and completeness. Using them, not only was a complete description of the evolution of the contracting body possible, but we've also obtained a description of the causal structure of the spacetime, in both regions.

The case of the thin shells, in particular, revealed the most simplicity, owing to the flat spacetime in the interior. Nevertheless, the features of the collapse are seen to be the similar. As such, thin shells are a reliable first approximation to gauge the general features of analogous collapsing bodies.

The thin shell formalism were also found to provide interesting limiting cases. The unbound and bound collapsing shell approximated converging flashes of light in the limits $m \to 0$ and $m \to \infty$ respectively.

This work was carried out in the case of non-rotating, spherically symmetric, bodies and shells made of dust. There are then two natural paths one may take to generalize the results here obtained. One may consider distributions on non frictionless material, i.e. mass energy distributions with non zero pressures. Another case of interest is that in which the body, or shell, is rotating. In this case, Birkhoff's theorem states the exterior spacetime will be a Kerr spacetime. For these cases, the results here obtain correspond then to the $p \to 0$ and $j \to 0$ limits repsectively.

[1] A. Einstein, Sitz. Preuss. Akad. d. Wis., **1915**, 844 (1915)
[2] K. Schwarzschild, Sitz. Preuss. Akad. d. Wis., **1916**, 189 (1916)
[3] J. R. Oppenheimer and G. M. Volkoff, Phys. Rev. **55**, 374 (1939)
[4] J. R. Oppenheimer and H. Snyder, Phys. Rev. **56**, 455 (1939)
[5] R. C. Tolman, Proc. Natl. Acad. Sci. USA, **20**, 169 (1934)
[6] C. A. R. Herdeiro and J. P. S. Lemos, Gazeta de Física, **41**, 2 (2018), arXiv:1811.06587v2
[7] The Event Horizon Telescope Collaboration, ApJ, **875**, (2019), arXiv:1906.11238
[8] I. D. Novikov and V. Frolov, *Physics of Black Holes*, (Springer Netherlands, Netherlands, 1989)
[9] P. S. Joshi and N. Dadhich and R. Marteens, Phys. Rev. D, **65**, 101501 (2002), arXiv:gr-qc/0109051v2
[10] F. C. Mena and B. C. Nolan and R. Tavakol, Phys. Rev. D, **70**, 084030 (2004), arXiv:gr-qc/0405041v1
[11] M. W. Choptuik, Phys. Rev. D, **70**, 9 (1993)
[12] C. Gundlach and J. M. Martín-García, Living Rev. Rel., **10** 1, (2007), arXiv:0711.4620v1 [gr-qc]
[13] J. V. Rocha and M. Tomašević, Phys. Rev. D, **98**, 104063 (2018), arXiv:1810.04907v2 [gr-qc]
[14] G. Darmois, *Mémorial des Sciences Mathématiques: Les équations de la gravitation einsteinienne,* **XXV**, (L'Académie des Sciences de Paris, Paris, 1927)
[15] C. W. Misner and D. H. Sharp, Phys. Rev. B, **136**, 571 (1964)
[16] W. Israel, Il Nuovo Cimento B, **44**, 1 (1966)
[17] R. J. Adler and J. D. Bjorken and P. Chen and J. S. Liu, Am. J. Phys., **73**, 1148 (2005), arXiv:gr-qc/0502040
[18] D. Lynden-Bell and J. P. S. Lemos, Mon. Not. R. Astr. Soc., **233**, 197 (1988)
[19] J. P. S. Lemos and D. Lynden-Bell, Mon. Not. R. Astr. Soc., **240**, 317 (1989)
[20] W. Israel, Phys. Rev., **153**, 1388 (1967)
[21] E. Poisson, *A Relativist's Toolkit: The Mathematics of Black-Hole Mechanics*, (Cambridge University Press, Cambridge, 2007)
[22] D. M. Eardley and L. Smarr, Phys. Rev. D, **19**, 2239 (1979)
[23] S. W. Hawking and G. F. R. Ellis, *The Large Scale Structure of Space-Time*, (Cambridge University Press, Cambridge, 2010)